REGULARIZED SPATIOTEMPORAL DECONVOLUTION OF FMRI DATA USING GRAY-MATTER CONSTRAINED TOTAL VARIATION

Younes Farouj[1,3], F. Işık Karahanoğlu[2] and Dimitri Van De Ville[1,4]

[1] Medical Image Processing Lab (MIP:Lab), Institute of Bioengineering, EPFL, CH-1015 Lausanne, Switzerland
[2]MGH/HST Athinoula A. Center for Biomedical Imaging, Harvard Medical School, Boston, MA, USA
[3]University of Lyon; CREATIS; CNRS UMR 5220; Inserm U1044, Villeurbanne, France
[4] Department of Radiology and Medical Informatics, University of Geneva, CH-1211 Geneva, Switzerland

ABSTRACT

Resting-state fMRI provides challenging data that needs to be analyzed without knowledge about timing or duration of neuronal events. The "total activation" framework is one recent approach that combines temporal and spatial regularization to deconvolve the fMRI signals; i.e., undo them from the influence of the hemodynamic response. The temporal regularization is using generalized total variation that promotes piecewise constant signals of the deconvolved timecourses. In the original formulation, the spatial regularization is expressing ℓ_2-smoothness within regions of a predefined brain atlas. In this work, we replace the latter with 3-D total variation that constrained to the gray matter domain. This allows the recovery of activation clusters with sharp boundaries without any bias from the atlas' partitioning. We propose the corresponding variational formulation and optimization problem, together with results that demonstrate the feasibility of the proposed approach for both simulated and real fMRI data.

Index Terms— fMRI, total activation, sparsity, deconvolution.

1. INTRODUCTION

Functional magnetic resonance imaging (fMRI) allows to measure brain activity via the blood oxygenated level dependent (BOLD) signal [1]. The BOLD signal is an indirect measure of neural activity through neurovascular coupling, vascular response, and changes in the ratio of oxygenated and desoxygenated hemoglobin. The whole process can be modeled as a nonlinear dynamic system (i.e., the balloon-windkessel model [2]. Classical detection methods are conceived to fit the time courses of each voxel with respect to a predefined experimental paradigm. This includes regression techniques that have been predominating in fMRI analysis schemes. The need for exploring spontaneous activity gave rise to deconvolution techniques that can deal with any timing or duration of underlying activity [3].

The activation maps show a macro-scale behavior; i.e., groups of neighboring neurons are expected to show similar activity. This property was harnessed in [5] to develop the total activation (TA) framework. TA uses the generalized total variation (gTV) in the temporal domain, introduced in [6], to impose a block-type prior on the shape of the underlying activity-inducing (deconvolved) signal together with a spatial regularization term promoting smooth activity within predefined regions from a structural atlas. With the high variability of the anatomical brain structure across subjects and the increasing interest in studying the richness of resting-state networks [4], it is valuable to construct methods that cannot be biased by atlas-based partitioning of the brain. Therefore, the present paper introduces an important improvement over the TA framework. Specifically, we couple the temporal gTV regularization with a spatial TV regularization restricted to voxels within the gray matter (GM) domain. Beyond the fact that this allows performing spatio-temporal deconvolution without spatial priors, the proposed approach has two other advantages compared to conventional TA: (1) it exploits the GM structure in the sense that the spatial regularization is not perturbed by voxels which are not suspicious to contribute to the activity; (2) processing only GM voxels and solving TV via proximal algorithms lead to a considerable gain in computational time. The rest of the paper is organized as follows. The fMRI BOLD signal model is presented in section 2. In section 3, we describe the proposed atlas-free spatio-temporal deconvolution technique along with the dedicated generalized forward-backward algorithm. Finally, we provide experimental results on synthetic and real data in section 4.

2. MODELING

We start by stating some classical assumptions about the fMRI signal. The acquired fMRI data is a set of voxels' time courses, $\mathbf{y}$, that are noisy and sampled versions of the BOLD activity-related signal, $\mathbf{x}$: $\mathbf{y}[v,t] = \mathbf{x}[v,t] + \varepsilon$, where $\{\varepsilon\}$ are random noise and nuisance components (such as low frequency fluctuations, signal drift, residual errors from motion correction, etc.). Throughout the paper, we denote by N_x and N_t, respectively, the number of voxels and the length of each time course. We consider that $\mathbf{x}$ describes the BOLD activation under the action of a linear time-invariant system $\mathcal{H}$ characterized by its impulse response, $\mathbf{h}$, the haemody-

This work was supported in part by each of the following: Région Rhône-Alpes (ARC 6), Bertarelli Foundation and SNF grant number P2ELP2_158891.

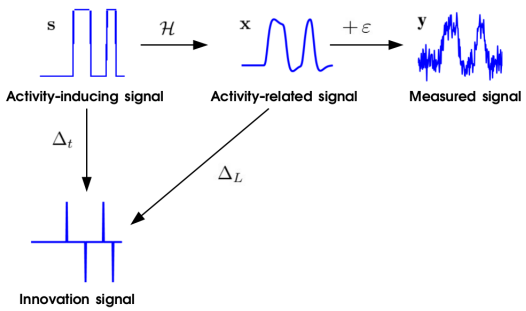

Fig. 1: The actions of the different operators on the different signals.

namic response function (HRF), in the following manner: $\mathbf{x}[v,t] = \sum_{\tau=0}^{t} \mathbf{s}[v,\tau]\,\mathbf{h}(t-\tau)$, where the activity-inducing signal, $\mathbf{s}$, describes the changes induced by the neural activity. In the sequel, we will make the following assumptions: (1) $\mathbf{s}$ is piece-wise constant; that is, the signal represents moments of sustained activation or deactivation; (2) the HRF, $\mathbf{h}$, is modeled by first-order Volterra series approximation of the balloon model [7]; (3) the noise component ε is white Gaussian. Assumption (1) means that the signal $\mathbf{s}$ is block-type; its derivative (in the finite difference sense) $\Delta_t\{\mathbf{s}\}$ is a sparse signal composed of Dirac pulses. Assumption (2) is also of particular interest as it facilitates the inversion of $\mathcal{H}$. In fact, Khalidov *et al.* [7] described the inverse $\mathcal{H}^{-1}$ as a closed form differential operator characterized by a gain $G \in \mathbb{R}_+$, one pole $\gamma \in \mathbb{C}_*$ and four zeros $(\alpha_1,\alpha_2,\alpha_3,\alpha_4) \in \mathbb{C}_*^4$: $\mathcal{H}^{-1} = \Big(\prod_{i=1}^{4}(D-\alpha_i I)\Big)\Big(D-\gamma I\Big)^{-1}$, with D, the continuous-domain derivation operator. Assumptions (1) and (2) are crucial for the construction of the temporal regularization because they allow us to impose a sparsity-promoting prior through the gTV. Assumption (3), which is widely used in fMRI, justifies the the use of a simple L^2-norm as a data-fidelity term.

3. ATLAS-FREE SPATIO-TEMPORAL DECONVOLUTION

Similarly to the work in [5], we use a spatio-temporal regularization to recover the activity-related signal, $\mathbf{x}$. In the sequel $\mathcal{R}_T$ and $\mathcal{R}_S$ will refer to the the temporal and spatial regularization terms, respectively. The variational formulation of this problem reads

$$\widehat{\mathbf{x}} = \arg\min_{\mathbf{x}} \left\{ \frac{1}{2}||\mathbf{y}-\mathbf{x}||_2^2 + \mathcal{R}_T(\mathbf{x}) + \mathcal{R}_S(\mathbf{x}) \right\}. \quad (1)$$

We start by describing the temporal regularization term which uses the concept of gTV. Afterwards, we describe the proposed GM-driven TV-based spatial regularization.

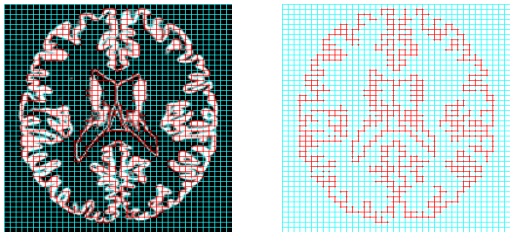

Fig. 2: Conceptual 2D-view on gray-matter grid (right) that is derived from the anatomical segmentation (left).

3.1. Temporal regularization $\mathcal{R}_T$

While conventional TV-regularization computes the ℓ_1-semi norm of the output of the finite difference operator, the gTV-regularization generalizes this concept to a larger class of differential operators. For our particular problem, we want to impose sparsity on the $\Delta_t\{\mathbf{s}\}$ while recovering $\mathbf{x}$. This simply suggests using a differential operator L whose discrete version Δ_L verifies $\Delta_L\{\mathbf{x}\} = \Delta_t\{\mathbf{s}\}$. We conclude that $\Delta_L = \Delta_t\mathcal{H}^{-1}$. In the continuous domain, this means that L has the same poles and zeros as $\mathcal{H}^{-1}$ with an additional null zero. We refer to [6] for details on the implementation of Δ_L from the knowledge of L. Fig. 1 summarize the actions of the different operators on the different signals. For each voxel $v = 1,\cdots,N_x$, the generalized TV corresponding to L reads:

$$TV_L\{\mathbf{x}\}[v] = \sum_{t=1}^{N_t} |\Delta_L\{\mathbf{x}\}[v,t]|\,.$$

Finally, the global temporal regularization is the sum of the generalized TV regularization terms over all voxels:

$$\mathcal{R}_T(\mathbf{x}) = \sum_{v=1}^{N_x} \lambda_T(v)\, TV_L\{\mathbf{x}\}[v], \quad (2)$$

where $\lambda_T(v)$ is the regularization parameter for voxel v.

3.2. Spatial regularization $\mathcal{R}_S$

The main purpose of this paper is to perform the deconvolution without imposing a predefined spatial partitioning of GM. We expect, however, that the activation take place in localized clusters of the brain with possibly sharp variations between them. Here, we use a TV-regularization restricted to voxels that can be activated; i.e., inside the GM domain. The idea of obtaining more robustness by adapting the analysis to the GM domain was exploited, for instance, in the context of wavelet-based SPM [8]. Fig. 2 shows a coarse view of how the finite difference grid is restricted to the GM map. At a fixed time point t, we define:

$$TV^{GM}\{\mathbf{x}\}[t] = \sum_{v=1}^{N_x} \left(\sum_{u\in\mathcal{N}(v)} \Big(\mathbf{x}[v,t]-\mathbf{x}[u,t]\Big)^2 \right)^{1/2},$$

where $\mathcal{N}(v)$ denotes the set of neighbor voxels around v, on the finite differences grid, that are within GM. Here again, the spatial regularization is the sum of the GM-driven TV-regularization terms over all time points:

$$\mathcal{R}_S(\mathbf{x}) = \sum_{t=1}^{N_t} \lambda_S(t)\, TV^{GM}\{\mathbf{x}\}[t], \tag{3}$$

with $\lambda_S(t)$ is the spatial regularization parameter at a given time point t.

3.3. Generalized foward-backward splitting

Both $\mathcal{R}_T$ and $\mathcal{R}_S$ are non-differentiable, but simple; their *proximal operators* [9] are easy to compute. The generalized forward-backward (GFB) proximal splitting [10] can be applied here to find a solution to (1). It consists of a weighted average of solutions to (1) with one regularization term at a time. The routine is given in Algorithm 1. Many choices are possible to deal with steps 1 and 2 of the main iteration. Here, we choose to employ internal FISTA [11] iterations for both problems. We refer to [6] for detailed explanation on how to adapt it to the gTV settings.

Algorithm 1 GFB algorithm for solving (1)

Input: Corrupted data $\mathbf{y}$, $(\omega_t, \omega_s) \in [0,1]^2$ with $\omega_1 + \omega_2 = 1$ and the operator L.
Output: Estimate $\widetilde{\mathbf{x}}$
for $k = 1 : k_{max}$ **do**
1: $\mathbf{x}_t^k = \arg\min_{\mathbf{x}} \left\{ \frac{1}{2}||\mathbf{y} - \mathbf{x}||_2^2 + \mathcal{R}_T(\mathbf{x}) \right\}$,
2: $\mathbf{x}_s^k = \arg\min_{\mathbf{x}} \left\{ \frac{1}{2}||\mathbf{y} - \mathbf{x}||_2^2 + \mathcal{R}_S(\mathbf{x}) \right\}$,
3: $\mathbf{x}^k = \omega_t \mathbf{x}_t^k + \omega_s \mathbf{x}_s^k$
end for
$\widetilde{\mathbf{x}} = \mathbf{x}^{k_{max}}$

4. EXPERIMENTS & DISCUSSION

In this section we present some experiments to assess the performance of the atlas-free spatio-temporal deconvolution for both simulated and real data. In both cases, the temporal regularization parameter, $\lambda_T(v)$, was tuned for each voxel using the median absolute deviation of fine-scale 3^{th} order Daubechies wavelet coefficients. The spatial regularization parameter was found empirically for each case. Values of $\omega_t = 0.75$ and $\omega_s = 0.25$ were used in all experiments.

4.1. Simulated data

To generate synthetic data, we used an activation map from FSL simulation tool (POSSUM[1]). This tool provides a 3D stationary signal intensity map generated from auditory naming tests [12]. We set this map in the range $[0, 3]$, at a resolution of $4 \times 4 \times 4$ mm^3, before multiplying it by a block-type signal of 200 s with 4 onsets (*cf.* Fig. 3). Finally, the obtained signals were convolved with the HRF (TR=2s) and perturbed by a white Gaussian random noise of unit variance. The measured PSNR on the final noisy time courses was 8.49 dB.

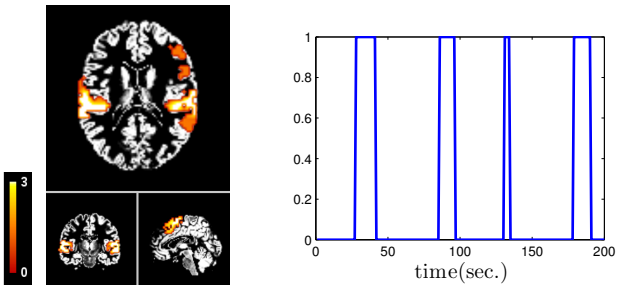

(a) (b)

Fig. 3: Ground truth for simulated data: (a) activation map, (b) experimental paradigm.

We applied both conventional TA and the proposed adaptation to retrieve the original signals from the noisy ones. To run conventional TA, we used the Harvard-Oxford atlas available in POSSUM. For both methods a value of $\lambda_S = 2$ was found to be a good compromise between noise suppression and signal preservation. The experiments were conducted using a PC with an Intel Core i7-3740QM CPU, 2.7 GHZ processor and 8 GB of RAM, using MATLAB v.8.2.0.701. The recorded run-time for TA was 5h53min while it was 4h30min for the atlas-free deconvolution. Fig. 4 reports the results. Both techniques succeeded at finding the evoked regions accurately. The proposed approach showed less artifacts outside the activation regions which leaded to a better PSNR. This is probably due to the local treatment provided by the restricted TV regularization. The denoised time courses show the good behavior of the proposed approach at keeping the signal close to the baseline when there is no activation.

4.2. Experimental data

To evaluate the atlas-free deconvolution in realistic conditions, we used experimental data acquired on a subject performing a task involving 9 visual stimuli (8 Hz flickering checkerboard). Each stimulus lasted 1s and its onset was randomly chosen following a uniform distribution. Inbetween visual stimuli events; the subject was asked to fix his/her eyes on the center of the screen. The fMRI data contains $N_t = 140$ $T2^*$-weighted gradient echo-planar volumes (TR/TE/FA = 2s/30ms/85^o, voxel size = $3.25 \times 3.25 \times 3.5$ mm^3). The first 10 volumes were removed to ensure a stable magnetic field, the time courses were realigned to correct for head motion, high pass filtered and smoothed in the spatial domain via a 3D Gaussian filter (FWHM = 5 mm). In order to downsample the GM resolution to the functional resolution, we used a

[1] http://fsl.fmrib.ox.ac.uk/fsl/fslwiki/POSSUM/UserGuide

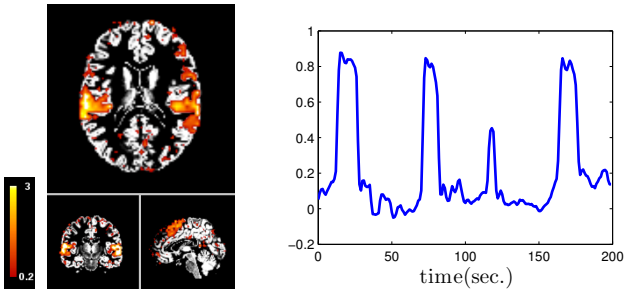

TA (19.89 dB)

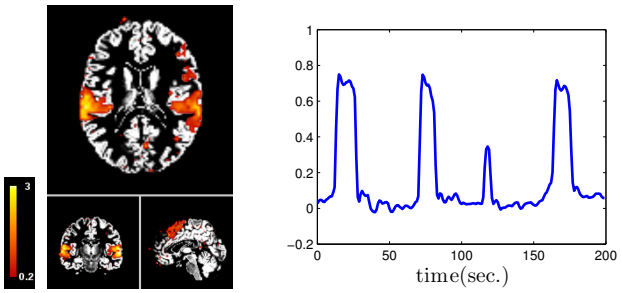

Atlas-free deconvolution (22.50 dB)

Fig. 4: Reconstructed activity-related signals **x** for TA and the atlas-free deconvolution. Left, volumetric view at the 2^{nd} activation; right, denoised time course of a voxel located in the auditory cortex. The PSNR was measured on all time courses within GM.

trilinear interpolation step followed by thresholding (threshold value 0.5). Fig. 5 displays the activity-inducing signal, **s**, and its average inside a small region of $6\times6\times6$ mm^3, located in the primary visual cortex. The structure of the visual cortex was well recovered without any spatial prior. The restored time course shows a perfect fit with the experiments. Negative values appearing in the signal are due to deactivations and/or the post-stimulus undershoot expressed in the HRF. Large negative values might indicate that the actual haemodynamic response is slower than the HRF model.

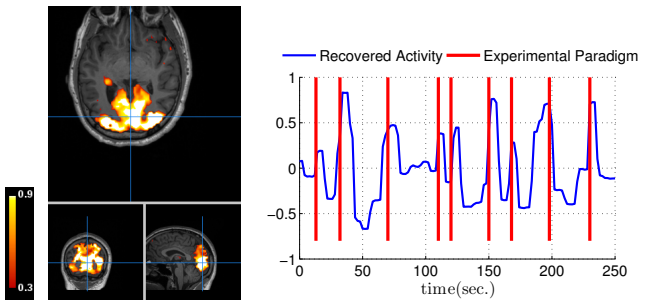

(a) (b)

Fig. 5: Reconstructed activity patterns ($\lambda_S = 5$): (a) positive values of the activity-inducing signal **s** at a time-point during the 2^{nd} activation, (b) the average of **s** inside the region indicated by the crossbars.

5. CONCLUSION

We showed that spatio-temporal deconvolution of fMRI data can be performed without incorporating priors on the timing, durations and atlas-based spatial structure of the activation. The results confirmed that a global regularity measure, such as TV, is able to retrieve localized activation clusters. Moreover, by adapting the spatial regularization inside GM we were able to add more robustness to the deconvolution while reducing the running time of the algorithm. Future work will focus on incorporating more sophisticated similarity measures between voxels by accounting for their proximity to brain's white matter and joint estimation of the activity-related signal and the HRF. The method will also be applied to large datasets of resting-state fMRI to obtain innovation-driven co-activation patterns [13].

6. REFERENCES

[1] S. Ogawa, T.-M. Lee, A. R. Kay, and D. W. Tank, "Brain magnetic resonance imaging with contrast dependent on blood oxygenation," *PNAS*, vol. 87, no. 24, pp. 9868–9872, 1990.

[2] R. B. Buxton, K. Uludağ, D. J. Dubowitz, and T. T. Liu, "Modeling the hemodynamic response to brain activation," *Neuroimage*, vol. 23, pp. S220–S233, 2004.

[3] C. C.-. Gaudes, N. Petridou, S. T. Francis, I. L. Dryden, and P. A. Gowland, "Paradigm free mapping with sparse regression automatically detects single-trial functional magnetic resonance imaging blood oxygenation level dependent responses," *Human brain mapping*, vol. 34, no. 3, pp. 501–518, 2013.

[4] S. M. Smith, K. L. Miller, S. Moeller, J. Xu, E. J. Auerbach, M. W. Woolrich, C. F. Beckmann, M. Jenkinson, J. Andersson, M. F. Glasser *et al.*, "Temporally-independent functional modes of spontaneous brain activity," *PNAS*, vol. 109, no. 8, pp. 3131–3136, 2012.

[5] F. I. Karahanoğlu, C.-. Gaudes, F. Lazeyras, and D. Van De Ville, "Total activation: fmri deconvolution through spatio-temporal regularization," *Neuroimage*, vol. 73, pp. 121–134, 2013.

[6] F. I. Karahanoğlu, İ. Bayram, and D. Van De Ville, "A signal processing approach to generalized 1-d total variation," *IEEE Trans. on Signal Process.*, vol. 59, no. 11, pp. 5265–5274, 2011.

[7] I. Khalidov, J. Fadili, F. Lazeyras, D. Van De Ville, and M. Unser, "Activelets: Wavelets for sparse representation of hemodynamic responses," *Signal Processing*, vol. 91, no. 12, pp. 2810–2821, 2011.

[8] H. Behjat, N. Leonardi, L. Sörnmo, and D. Van De Ville, "Anatomically-adapted graph wavelets for improved group-level fmri activation mapping," *NeuroImage*, vol. 123, pp. 185–199, 2015.

[9] J.-J. Moreau, "Proximité et dualité dans un espace hilbertien," *Bull. de la Société math. de France*, vol. 93, pp. 273–299, 1965.

[10] H. Raguet, J. Fadili, and G. Peyré, "A generalized forward-backward splitting," *SIAM Journal on Imaging Sciences*, vol. 6, no. 3, pp. 1199–1226, 2013.

[11] A. Beck and M. Teboulle, "A fast iterative shrinkage-thresholding algorithm for linear inverse problems," *SIAM journal on imaging sciences*, vol. 2, no. 1, pp. 183–202, 2009.

[12] I. Drobnjak, D. Gavaghan, E. Süli, J. Pitt-Francis, and M. Jenkinson, "Development of a functional magnetic resonance imaging simulator for modeling realistic rigid-body motion artifacts," *Magnetic Resonance in Medicine*, vol. 56, no. 2, pp. 364–380, 2006.

[13] F. I. Karahanoğlu and D. Van De Ville, "Transient brain activity disentangles fmri resting-state dynamics in terms of spatially and temporally overlapping networks," *Nature communications*, vol. 6, 2015.